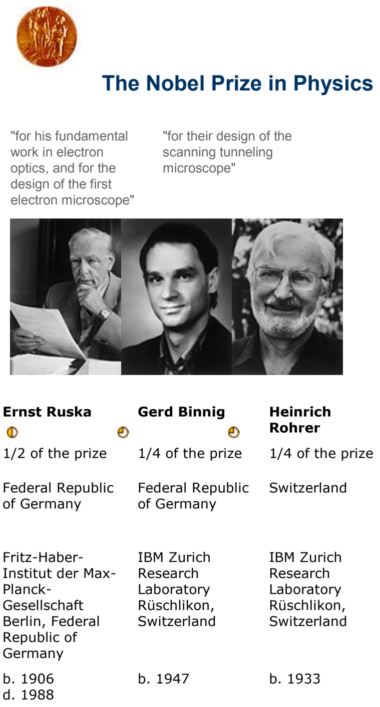

The Nobel Prize in Physics 1986

"for his fundamental work in electron optics, and for the design of the first electron microscope"

"for their design of the scanning tunneling microscope"

Ernst Ruska	**Gerd Binnig**	**Heinrich Rohrer**
1/2 of the prize	1/4 of the prize	1/4 of the prize
Federal Republic of Germany	Federal Republic of Germany	Switzerland
Fritz-Haber-Institut der Max-Planck-Gesellschaft Berlin, Federal Republic of Germany	IBM Zurich Research Laboratory Rüschlikon, Switzerland	IBM Zurich Research Laboratory Rüschlikon, Switzerland
b. 1906 d. 1988	b. 1947	b. 1933

Microscopy is the science of seeing the very small. Under ideal conditions, the eye resolves about 1 minute of arc (= 1/60 degree = 2.9x10-4 radian; recall there are 2p radians in 360°) and since it can focus down to about 250mm, the smallest object we can resolve is about 0.07mm (70mm) (Fig. I.14). This limit is related to the size of the receptors in the retina of the eye. The <u>function of a microscope</u> is to <u>magnify the image falling on the retina</u> (Fig. I.15). The advantage of light and electron microscopes is that they effectively get the object closer to the eye so a magnified image is obtained and more detail can be discerned.

DATE	NAME	EVENT
1897	J. J. Thompson	Discovers the electron
1924	Louis deBroglie	Identifies a wavelength to moving electrons $\lambda=h/mv$ where λ = wavelength h = Planck's constant m = mass v = velocity (For an electron at 60kV λ = 0.005 nm)
1926	H. Busch	Magnetic or electric fields act as lenses for electrons
1929	E. Ruska	Ph.D thesis on magnetic lenses
1931	Knoll & Ruska	First electron microscope built
1931	Davisson & Calbrick	Properties of electrostatic lenses
1934	Driest & Muller	Surpass resolution of the LM
1938	von Borries & Ruska	First practical EM (Siemens) - 10 nm resolution
1940	RCA	Commercial EM with 2.4 nm resolution
1945		1.0 nm resolution

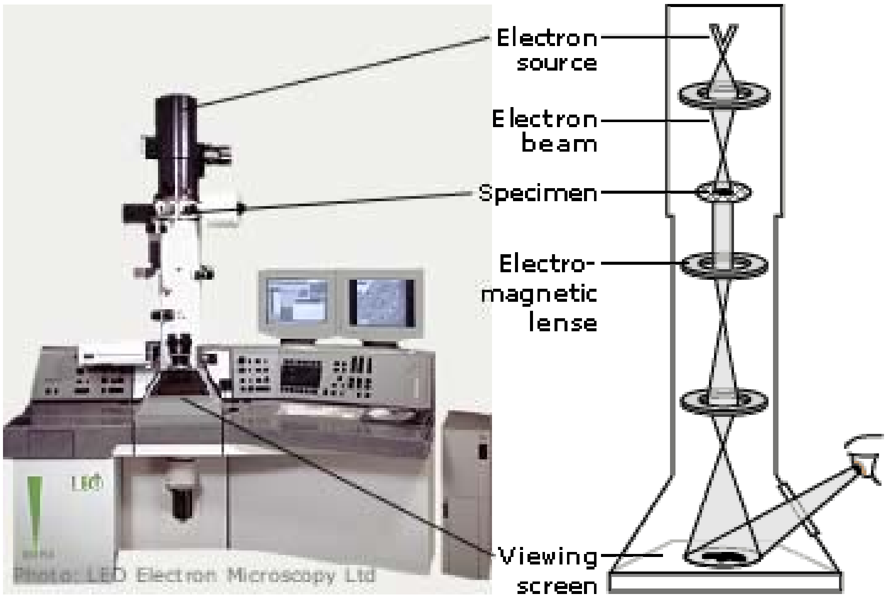

http://www.mwrn.com/guide/electron_microscopy/microscope.htm

http://em-outreach.ucsd.edu/web-course/toc.html http://www.matter.org.uk/tem/

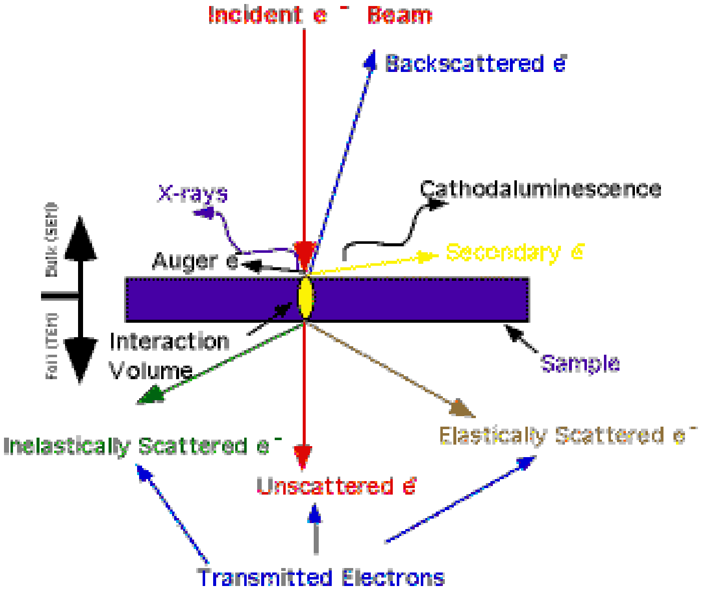

Thermionic electron gun

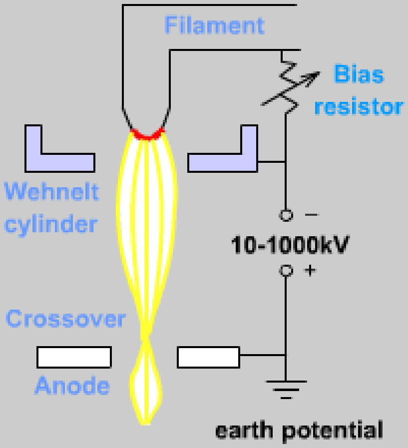

The ***filament*** is made from a high melting point material of relatively low work function, ϕ in order to emit many electrons. Common choices are:

- Tungsten: ϕ = 4.5 eV
- Lanthanum hexaboride: ϕ = 3.0 eV

Click here for a photo of a real filament.

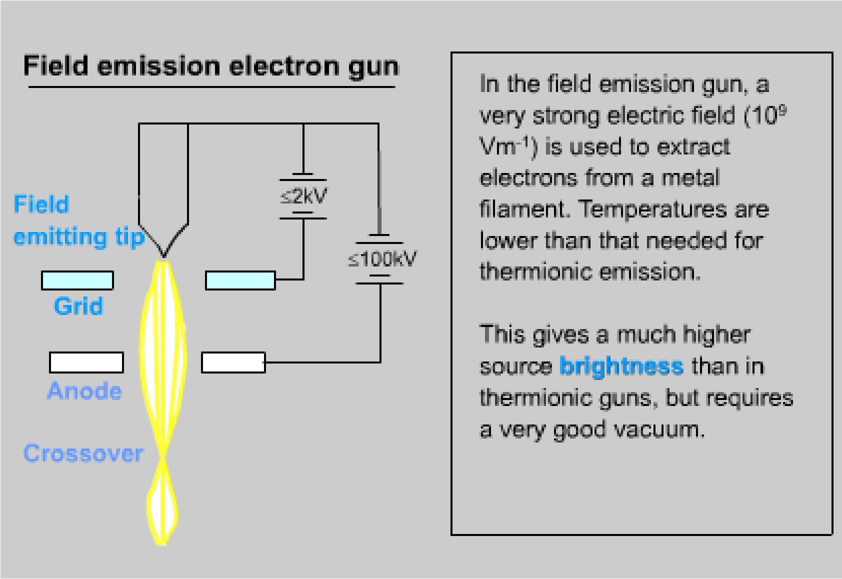

Field emission electron gun

In the field emission gun, a very strong electric field (10^9 Vm^{-1}) is used to extract electrons from a metal filament. Temperatures are lower than that needed for thermionic emission.

This gives a much higher source **brightness** than in thermionic guns, but requires a very good vacuum.

The actual beam diameter results from the diameter of the original beam leaving the electron gun, d_g broadened by the effect of spherical aberation in the lenses d_s and diffraction at the aperture, d_d. These depend on the current, *i*, convergence angle, α, brightness, β, spherical aberation coefficient, C_s, and wavelength, λ, via

$$d_g = \frac{2}{\pi}\sqrt{\frac{i}{\beta}}\frac{1}{\alpha} \qquad d_s = 0.5C_s\alpha^3 \qquad d_d = 1.22\frac{\lambda}{\alpha}$$

The total beam diameter is found by adding these three effects in quadrature i.e.

$$d_t = \sqrt{d_s^2 + d_g^2 + d_d^2}$$

Non-Relativistic Electron

$$\lambda = \frac{h}{mv} \qquad \tfrac{1}{2}mv^2 = eV \qquad v = \sqrt{\frac{2eV}{m}}$$

$$\lambda = \left(\frac{h}{m}\right) * \frac{1}{\sqrt{\frac{2eV}{m}}} = \sqrt{\frac{h^2}{2meV}} \qquad \lambda = \sqrt{\frac{150}{V}} * 10^{-8}\, cm = \frac{1.23}{\sqrt{V}}\, nm \qquad v = 0.593 \times 10^8 \sqrt{V} cm / \sec$$

V	λ (nm)	v (10^8 m/sec)	v/c
10,000	0.0123	0.593	0.198
50,000	0.0055	1.326	0.442
100,000	0.0039	1.875	0.625
1,000,000	0.0012	5.930	**1.977!**

Relativistic Electron

$$m_1 = \frac{m_0}{\sqrt{1 - \frac{v^2}{c^2}}} \qquad \lambda = \frac{1.23}{\sqrt{V + 10^{-6} V^2}}\, nm$$

V	λ (nm)	v (10^8 m/sec)	v/c
10,000	0.0122	0.584	0.195
50,000	0.0054	1.24	0.414
100,000	0.0037	1.64	0.548
1,000,000	0.0009	2.81	**0.941**

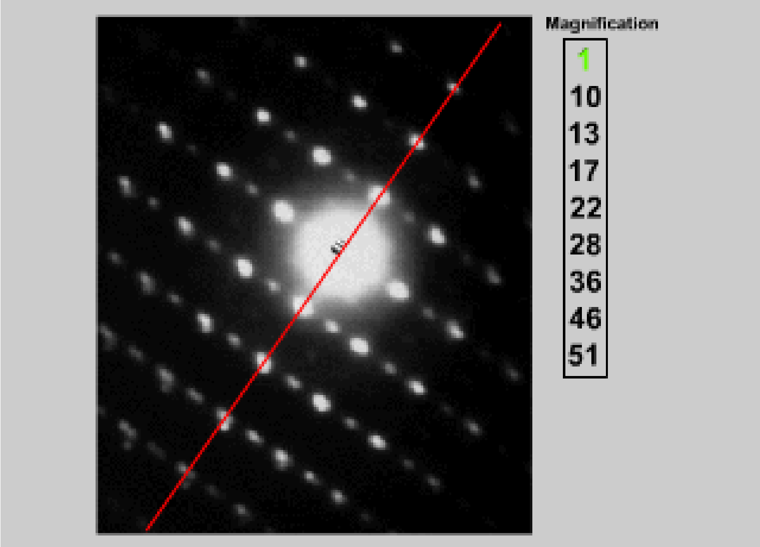

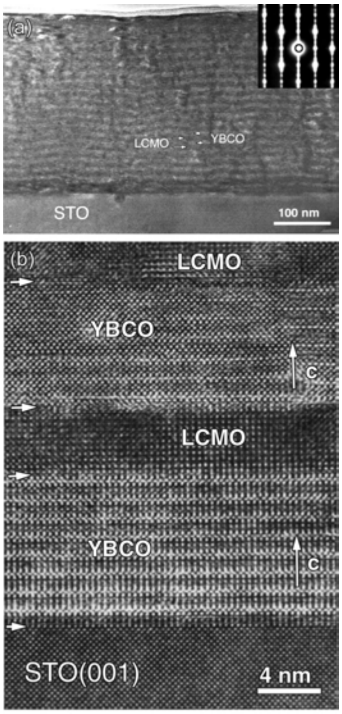
(a)
LCMO
YBCO
STO
100 nm
(b)
LCMO
YBCO
c
LCMO
YBCO
c
STO(001)
4 nm

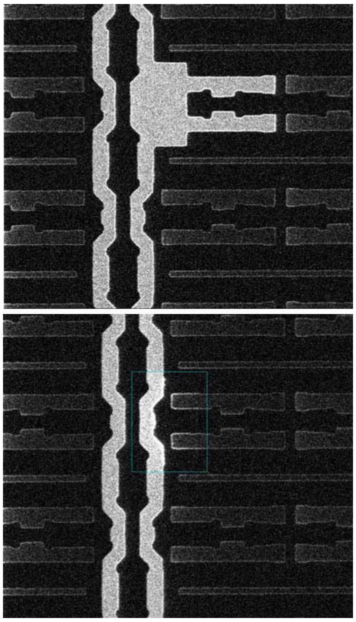

X-ray Emission

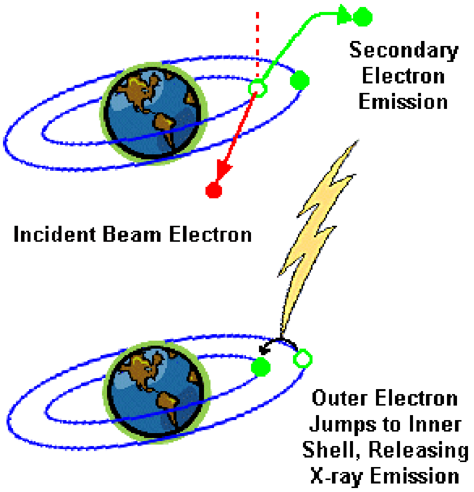

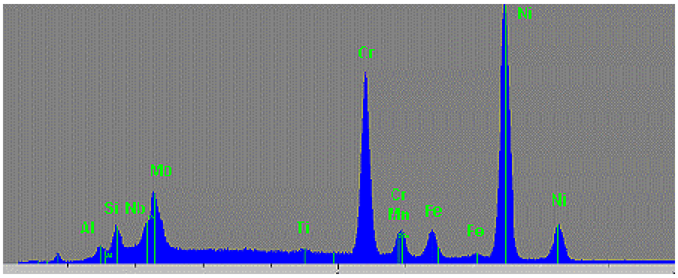

Element	Atomic %	Weight %
Al	2.588	1.203
Si	4.247	2.056
Ti	0.365	0.301
Cr	21.793	19.529
Mn	0.229	0.216
Fe	3.931	3.783
Ni	58.337	59.013
Nb	3.261	5.221
Mo	5.249	8.677

Scanning Electron Microscope

SEM Beam focusing

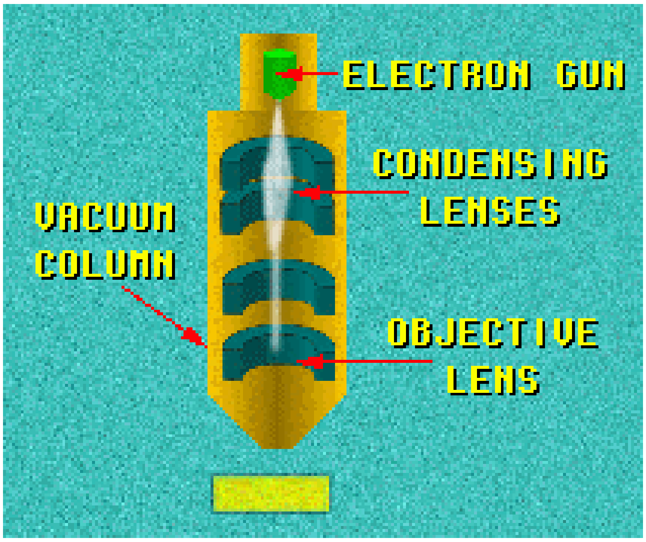

SEM Beam Scanning

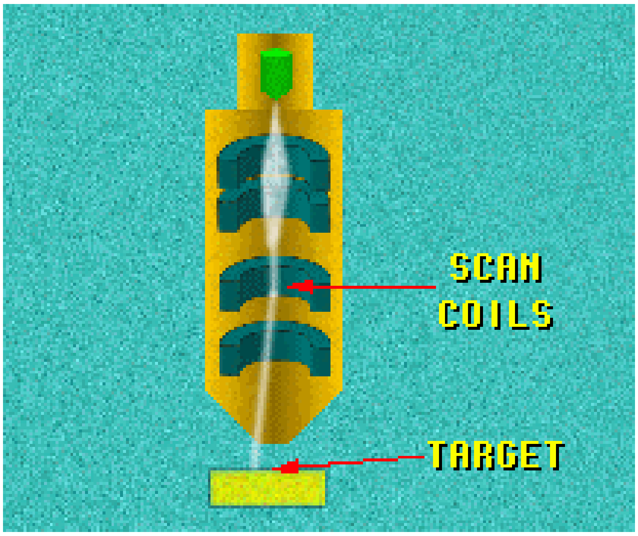

SEM Beam Dectection

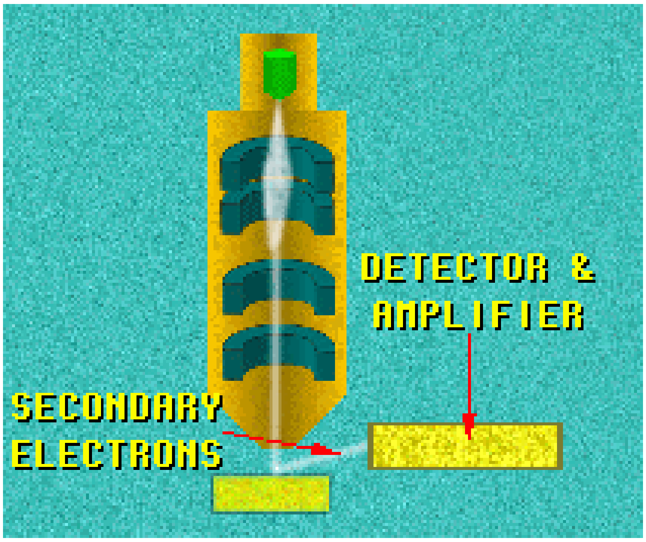

Gold Coated Mosquito Mounted

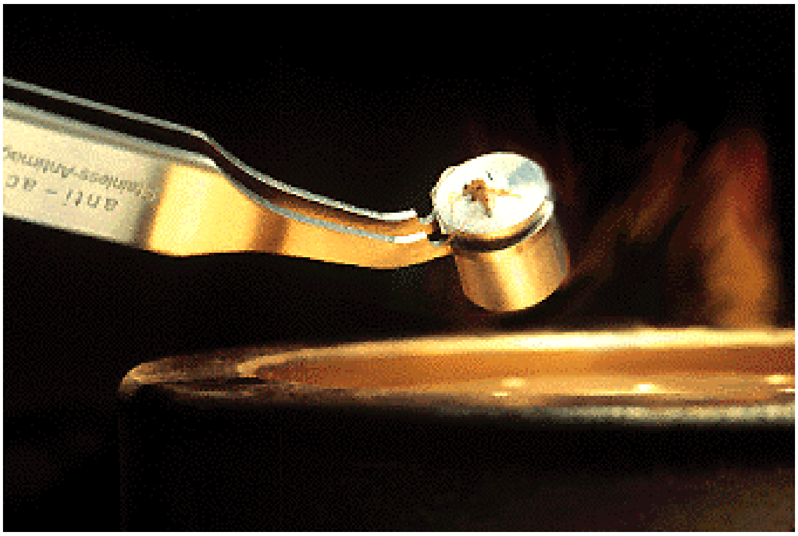

Mosquito X 35

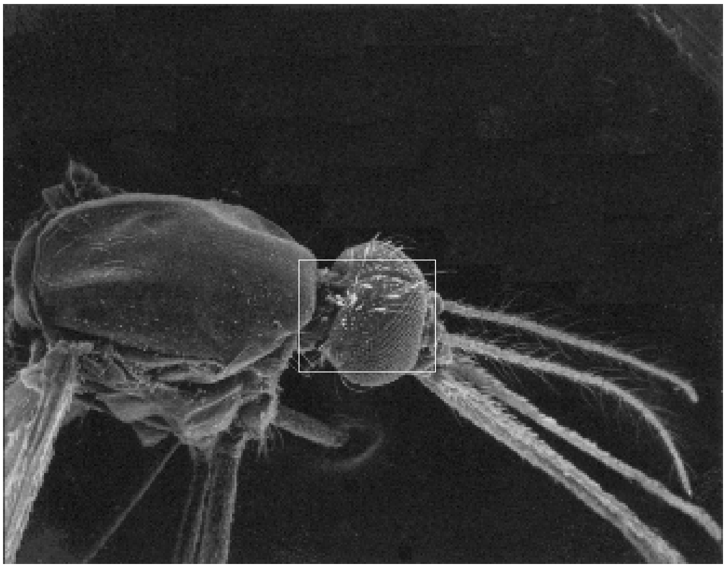

Mosquito X 200

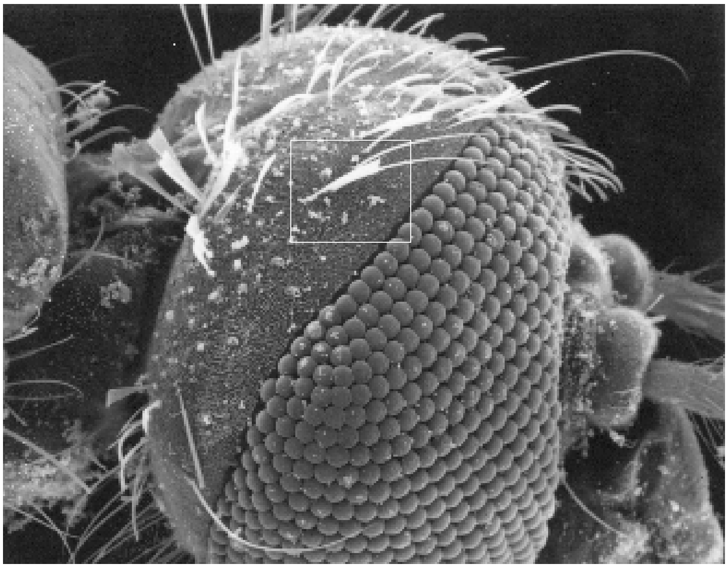

Mosquito X 1000

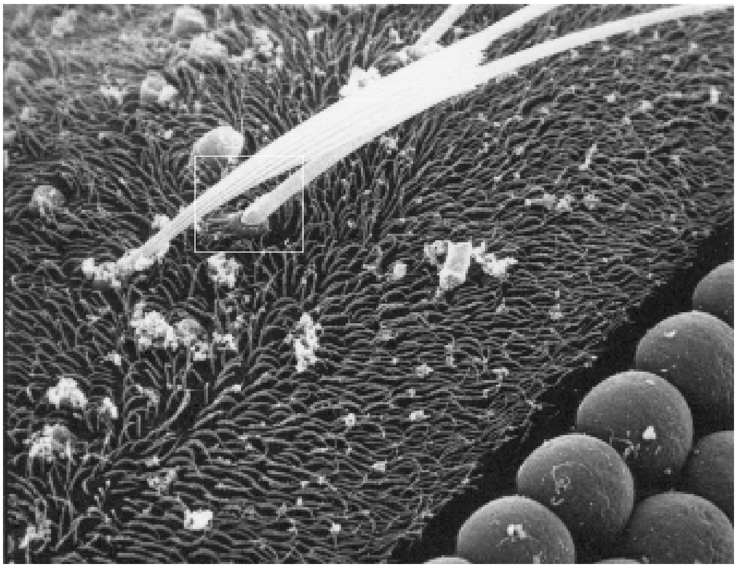

Mosquito X 5000

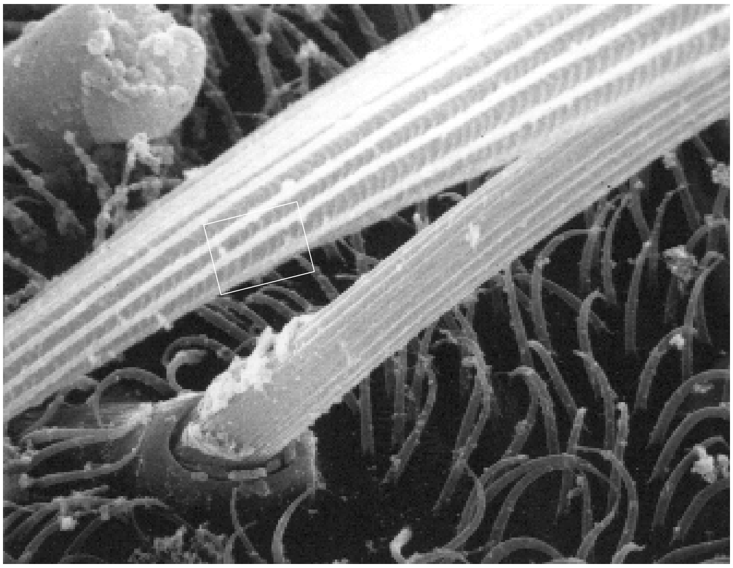

Mosquito X 35000

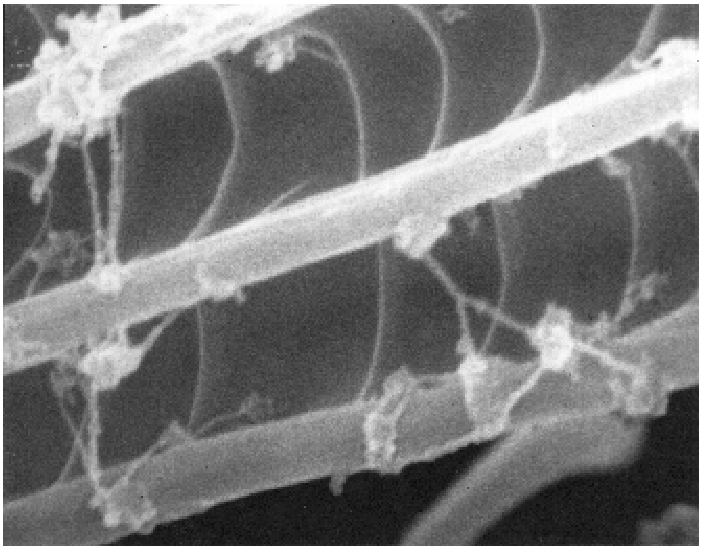

What is This?

What is This?

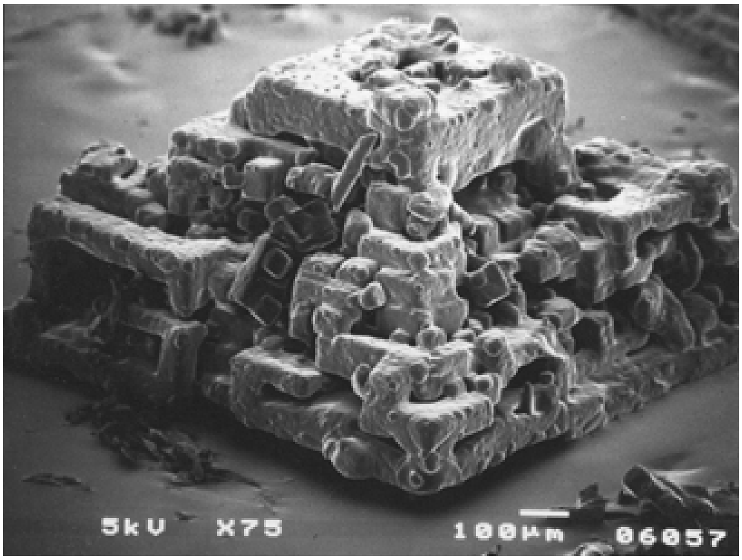

What is This?

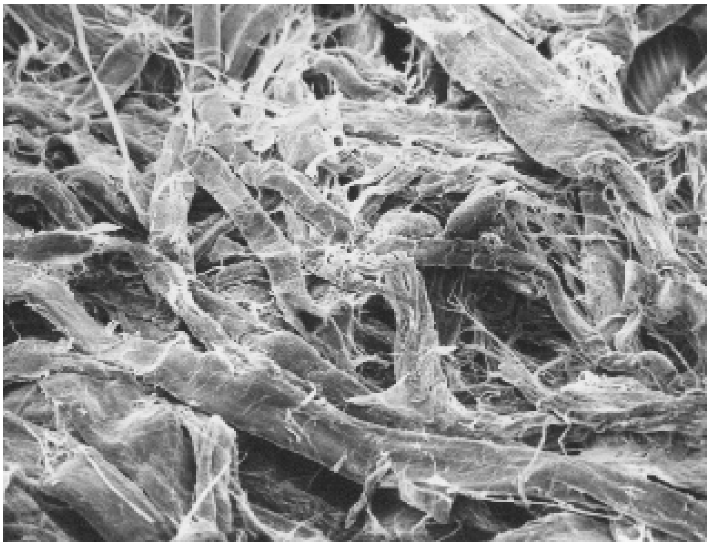

What is This?

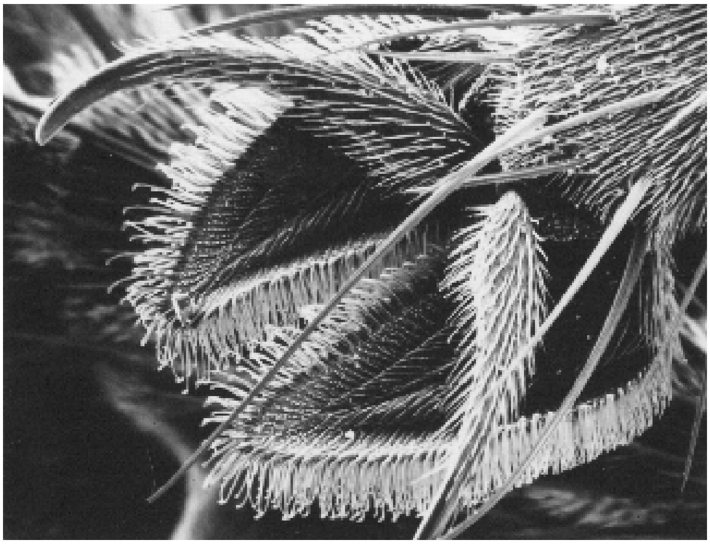

What is This?

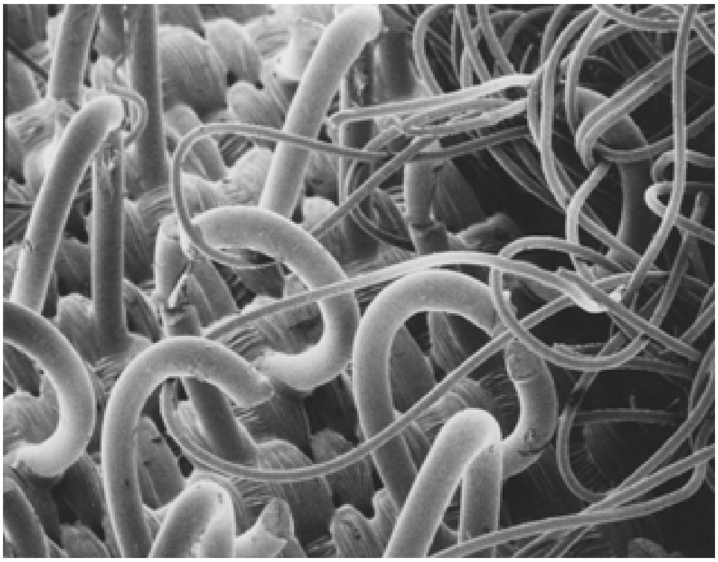

What is This?

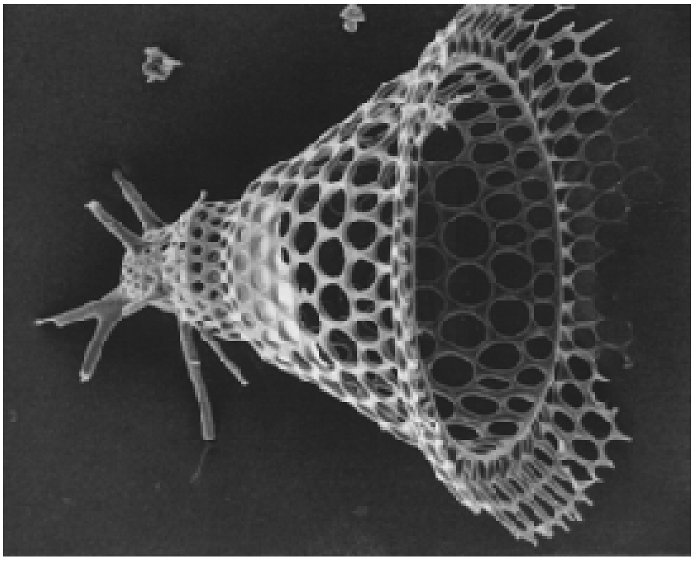

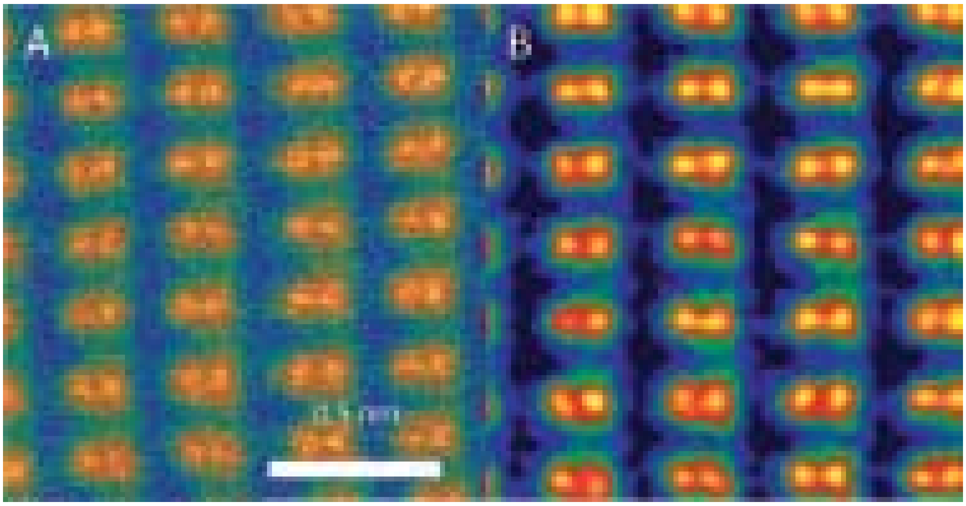

Looking straight down on a silicon crystal in the direction <112>, the atoms line up in closely-spaced pairs of columns with just 0.78 angstrom between each column in a pair. The dumbbell shape shows that the microscope has achieved better than 0.78 Angstrom resolution. With a smaller beam the rows would be seen as two clearly separated features, but with a larger beam the pair would blur into one oval-shaped feature. Analysis of the power spectrum shows the presence of information down to a record 0.6 angstrom. – P.D. Nellist, *et al.*, Science, **305**, 1741 (2004)

Electron Energy Loss Spectroscopy (EELS)

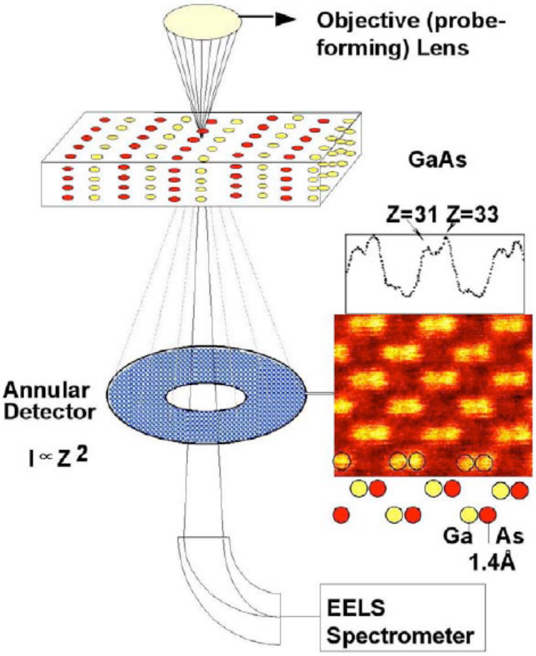

Electron Energy Loss Spectroscopy (EELS)

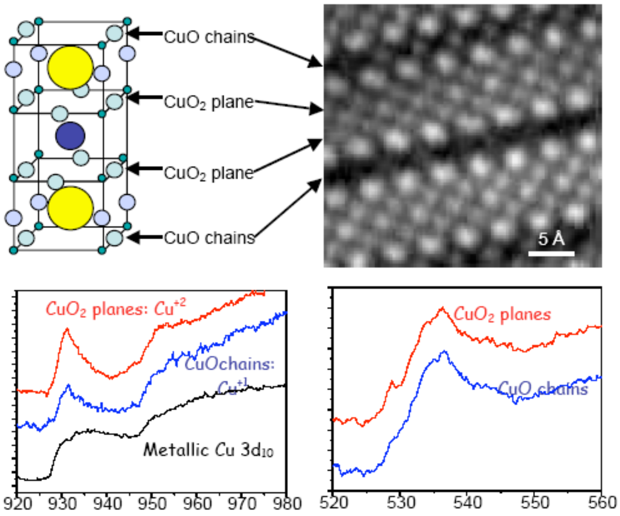

Fig. 5. Schematic of YBCO structure with Cu/O planes and chains arrowed in the Z-contrast image. Spectra obtained from the chains and planes separately show (left) their different $L_{2,3}$ ratio at the Cu edge, with metallic Cu as a reference, and (right) a prepeak in the O K edge region of the spectra indicating holes localized in the planes.

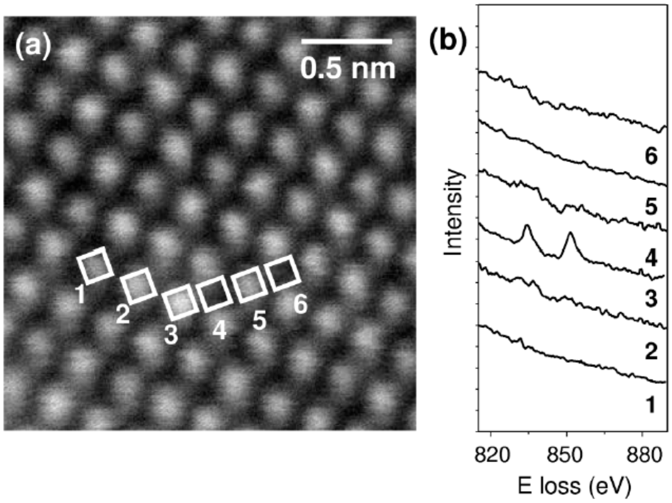

FIG. 2. (a) Z-contrast image with (b) EELS traces showing spectroscopic identification of a single La atom at atomic spatial resolution, with the same beam used for imaging. The $M_{4,5}$ lines of La are seen strongly in spectrum 3 obtained from the bright column at 2×10^7 magnification and a total collection time of 30 s. Other spectra from neighboring columns

M. Varela, *et al.*,
Phys. Rev. Lett. **92**,
095502 (2004)

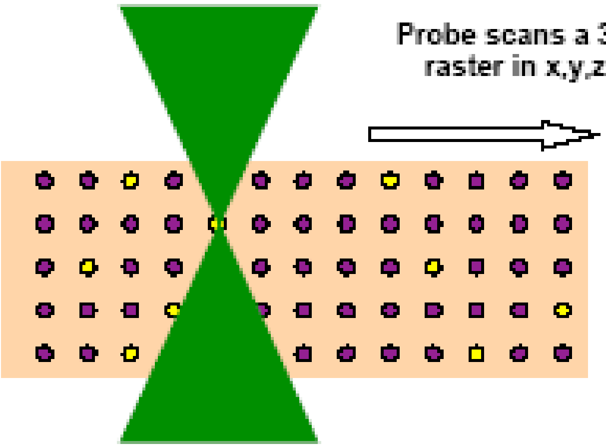

FIGURE 11. Schematic showing depth sectioning in the STEM. The impurity atoms (lighter) may be identified from the image or by spectroscopy and the entire specimen reconstructed at atomic resolution in 3D.

Scanning Tunneling Microscopy

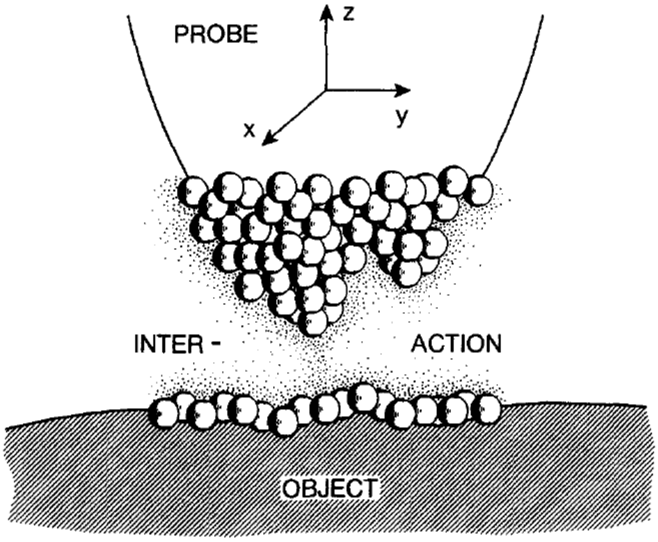

J.A. Kubby and J.J. Boland, Surf. Sci. Rep. **26** 61-204 (1996)

$$-(\hbar^2/2m)\psi'' + [V(x) - E]\psi = 0$$

has the solutions

$$\psi(x) = \begin{cases} Ae^{+ikx} + Be^{-ikx} & (x < 0), \\ Ce^{-\mathrm{k}x} + De^{+\mathrm{k}x} & (0 < x < s), \\ Fe^{+ikx} & (x < s), \end{cases}$$

where

$$\hbar k = (\,2mE)^{1/2}; \qquad \hbar\mathrm{k} = (2m[V_0 - E])^{1/2}.$$

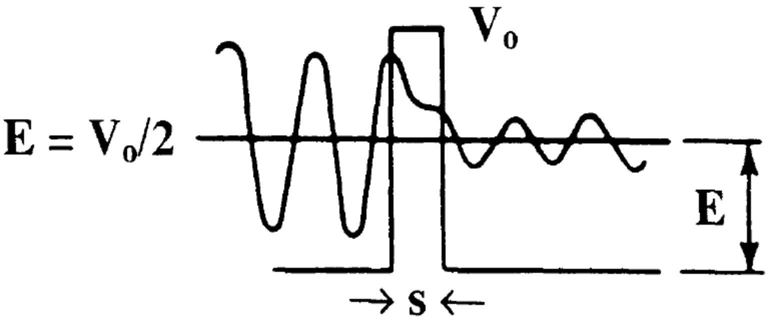

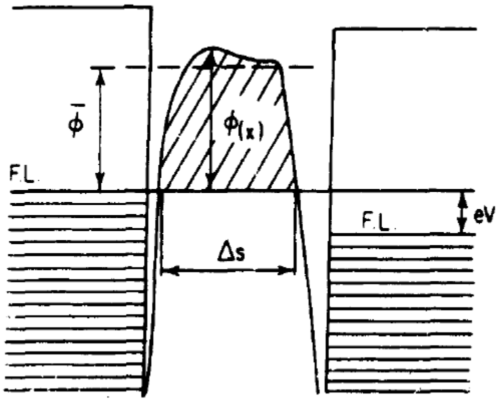
φ̄
φ(x)
F.L.
eV
F.L.
Δs

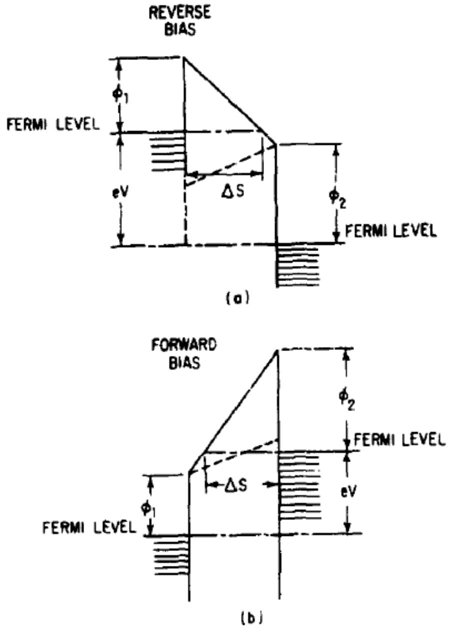
REVERSE BIAS
φ1
FERMI LEVEL
eV
ΔS
φ2
FERMI LEVEL
(a)
FORWARD BIAS
φ2
FERMI LEVEL
ΔS
eV
φ1
FERMI LEVEL
(b)

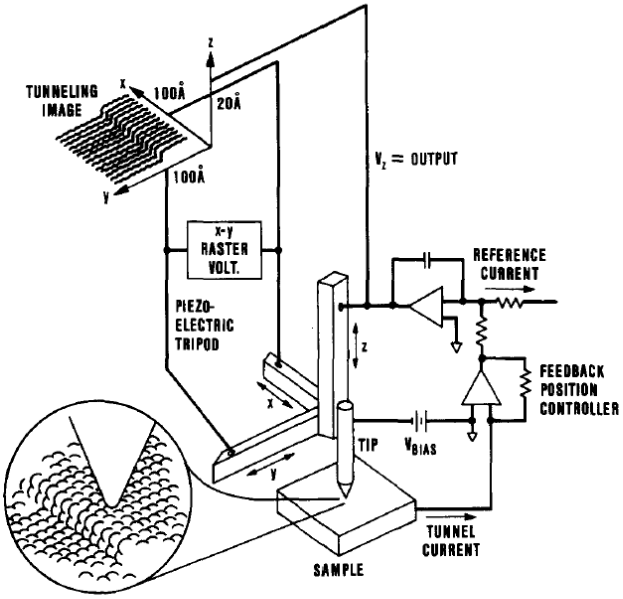
TUNNELING IMAGE
x
100Å
z
20Å
100Å
y
V_z = OUTPUT
x-y RASTER VOLT.
REFERENCE CURRENT
PIEZO-ELECTRIC TRIPOD
z
FEEDBACK POSITION CONTROLLER
x
y
TIP
V_{BIAS}
TUNNEL CURRENT
SAMPLE

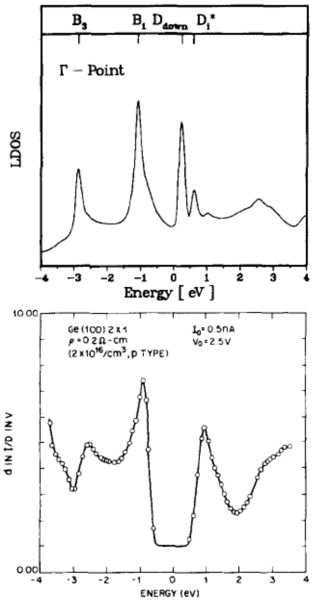
B_3
B_1
D_{down}
D_1^*
Γ – Point
LDOS
-4
-3
-2
-1
0
1
2
3
4
Energy [eV]
10.00
0.00
Ge (100) 2 x 1
ρ = 0.2 Ω-cm
(2×10^{16}/cm^3, p TYPE)
I_0 = 0.5nA
V_0 = 2.5V
d ln I/d ln V
-4
-3
-2
-1
0
1
2
3
4
ENERGY (eV)

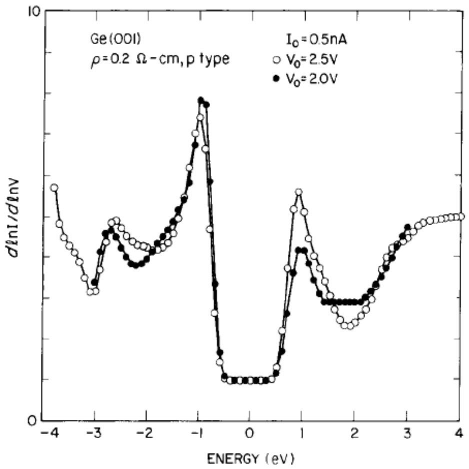

Fig. 82. Normalized conductance vs. bias voltage relative to the Fermi energy. Stabilization voltages of 2.0 and 2.5 V at a demanded tunneling current of 0.5 nA were used to obtain the spectra. The spectra shown are the average of 200 spectra. The occupied-state peak at −1 eV corresponds to the D_{up} (π-bonding) band, and the unoccupied-state peak at +0.9 eV corresponds to the D_{down} (π^*-anti-bonding) band. The energy scale is shown for sample bias [286].

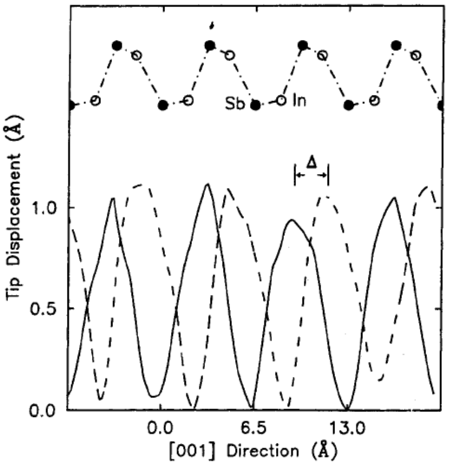

Fig. 111. A pair of STM profiles along the [001] direction of InSb(110) interpolated from two images acquired simultaneously at −1.5 V (solid line; antimony, filled states) and +1.35 V (dashed line; indium, empty states). The average displacement, Δ, of the antimony and indium state density is 2.4 ± 0.4 Å. A side view of the atomic structure of the top two surface layers as calculated by Mailhiot et al. [370] is shown for comparison (vertical dimensions not to scale) [369].

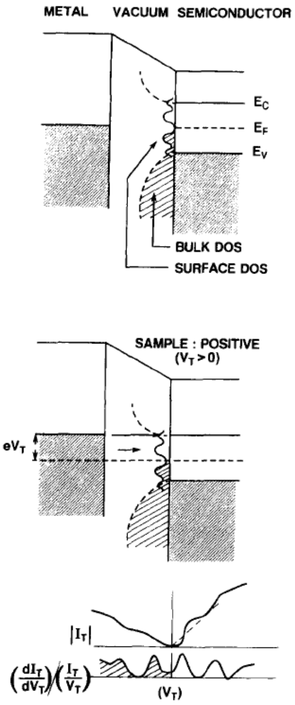

AFM Image of
InGaAs Quantum
Wires on GaAs